

## **Effect of Corrosion Behaviour of Laser Melted GP1 Stainless Steel**

Kurian Antony<sup>a\*</sup>, Siva Prasad M<sup>b</sup>, Ajith A<sup>a</sup>, Cijesh.T.John<sup>a</sup>, Deepu Mathew George<sup>a</sup>, George Benedict<sup>a</sup>

<sup>a</sup>Department of Mechanical Engineering, Amal Jyothi College of Engineering,  
Kanjirappally, Kerala, India 686518,

<sup>b</sup>Department of Metallurgy, Amal Jyothi College of Engineering,  
Kanjirappally, Kerala, India 686518

Corresponding Author: kurianantony@amaljyothi.ac.in

### **Abstract:**

This paper mainly focuses in the Hot corrosion test on laser sintered stainless steel GP1 powder using pulsed Nd: YAG laser. The objectives of this study were to analyze the microstructure characteristics and phase change of the laser melted stainless steel part. The investigation is to understand the effects of high temperature corrosion at various time cycles. The surface characteristics of hot corroded samples were methodically analyzed by tools like macro and microscopic inspection, X-Ray diffraction (XRD). The results presented in this paper are helpful to realize the hot corrosion in additive manufacturing processes involving powder melting by laser beam.

Keywords: Laser melting, stainless steel, high temperature corrosion, molten salt environment

### **1. Introduction**

Laser melting is an additive manufacturing process in which the components with complex shapes are formed directly from metallic powder Kurian et al. (2014). In laser melting process, parts are usually fabricated by melting a thin layer of metal powder on a substrate or previously formed layer using one or more laser beam [2].

Hot corrosion is the most aggressive method of degradation of metals, alloys and ceramics, especially when they operate at very high temperatures. Rapid degradation occurs due to lack of a solid layer found on the substrate [3].

Components that are affected by hot corrosion attack include gas turbines, industrial plants and jet engines. This can also be defined as the accelerated oxidation of materials that is induced by a film deposit of salt at elevated temperatures [4]. There are two types of hot corrosion: type I and type II. A type I hot corrosion attack happens at a temperature range of 800°C to 900°C, with the minimum threshold being the melting point of the salt deposit. The upper temperature is taken to be the salt dew point. This happens in two stages: an incubation period where the rate of attack is slow as the oxide layer forms, and then the rate accelerates quickly. The incubation period is related to the formation of a protective oxide scale. Initiation of accelerated corrosion attack is believed to be related to the breakdown of the protective oxide scale. Many mechanisms have been proposed to explain accelerated corrosion attack; the salt fluxing model is probably the most widely accepted. Oxides can dissolve in Na<sub>2</sub>SO<sub>4</sub> as anionic species (basic fluxing) or cationic species (acid fluxing), depending on the salt composition. Salt is acidic when it is high in SO<sub>3</sub>, and basic when low in SO<sub>3</sub> [5–7].

The selection of this powder material is motivated by the fact that among many stainless steel alloys, GP1 steel are versatile alloys having high corrosion resistance, formability, high strength, weld ability and biocompatibility which are suitable for orthopedic applications, such as implants and prosthesis, pharmaceuticals, architectural applications, fasteners, airframe and aircraft engine parts, marine chemical parts, condenser tubing, and heat exchanger. Several characterization tools are utilized to analyze the temperature distribution around the material. Additionally, the samples are characterized using XRD analysis to understand the process property structure relationship under laser melting and solidification and also the hot corrosion test.

## **2. Experimentation**

To facilitate the hot corrosion test, a laser melted specimen was cut into rectangular piece ( $20 \times 15 \times 5$  mm) and was mirror polished. To remove the moisture from the sample and also for the salt to adhere to the surface uniformly the sample is preheated to  $250\text{ }^{\circ}\text{C}$ . Immediately, a coating of uniform thickness with  $3\text{--}5\text{ mg/cm}^2$  of salt mixture was applied on the preheated sample. On this specimen, cyclic studies were performed in the air as well as molten salt ( $\text{K}_2\text{SO}_4\text{--}60\%\text{ NaCl}$ ) for exactly 10 cycles and the duration of each cycle is for 24 hours in which heating is for five hours at  $550\text{ }^{\circ}\text{C}$  in a furnace followed by 19 hours of cooling at room temperature. During the corrosion tests, the weight change measurements were taken at the end of each cycle. The spalled scale was also retained during the measurement of the weight change to determine the total rate of corrosion. The sample after corrosion tests was subjected to characterization studies using XRD for surface analysis of the scale. Here, on the laser sintered stainless steel specimen, different etchants were used and better results were obtained on use of aqua regia.

Some of the etchants used:

Acetal

Aqua Regia (  $4\text{HCl} + 1\text{HNO}_3$  )

Fry's Reagent (  $1\text{ g CuCl}_2, 25\text{ mL HCl}, 150\text{ mL H}_2\text{O}, 25\text{ mL HNO}_3$  )

#### **4. Results and discussions**

The surface morphological studies has been carried out and found that the metals and alloys undergo oxidation when exposed at elevated temperatures in air which may be may be protective or non-protective. Whereas the metals exposed in molten salt environment could accelerate the corrosion rate due to combined form of oxidation, chloridation and sulphidation. This leads to the formation of dark pits fig.1–3. At first cycle, for 24 hrs heating at the rate of  $550\text{ }^{\circ}\text{C}$  the formation of dark pits was noticed. However after second cycle descaling is clearly visible from the sample surface fig.3. Whereas in the third cycle the corrosion morphology of the material exposed in  $\text{K}_2\text{SO}_4\text{--}60\%\text{ NaCl}$

shows that the surface interface is more prone to formation of fragile scale fig.4. This implies that NaCl plays a vital role in hot corrosion. It is observed that, the corrosion rate in K<sub>2</sub>SO<sub>4</sub>-60% NaCl environment is higher in magnitude than air oxidation environments.

Figure 5 explains the weight gain per unit area versus function of time (number of cycles). These figures indicate that the weight gain kinetics under air oxidation shows a steady-state parabolic rate law, whereas the molten salt environment is a multi-stage weight-gain growth rate. It is noted that, the hot corrosion in molten salt environment was observed to be more extensive. Moreover, higher corrosion rate is observed during initial hours of study and is mainly attributed to the rapid oxygen pick up by diffusion of oxygen through the molten salt layer and is found to be identical to the results reported by Sidhu and Prakash [8], Tiwari and Prakash [9] during their hot corrosion studies. As revealed by XRD, different phases of various reaction products were formed on the surface after corrosion cycles. Hot corrosion under molten salt environment at 550 °C shows that Fe<sub>2</sub>O<sub>3</sub> and Cr<sub>2</sub>O<sub>3</sub> as the predominant phases and NiCr<sub>2</sub>O<sub>4</sub>, (Cr, Fe)<sub>2</sub>O<sub>3</sub>, FeNi and FeS are observed with low intensity.

Many researchers have pointed out that the formation of sodium chromate (Na<sub>2</sub>CrO<sub>4</sub>) could result from oxy-chloridation even the temperature is lower than the melting point of salt deposits [10–12]. As Na<sub>2</sub>CrO<sub>4</sub> is formed, the salt will wet the specimen surface which eventually leads to a mechanism of hot corrosion dominated by molten salt and is further validated by XRD analysis. The analysis of the scale shows predominant Fe<sub>2</sub>O<sub>3</sub> with low intensities of Cr<sub>2</sub>O<sub>3</sub>, Na<sub>2</sub>CrO<sub>4</sub>, SO<sub>3</sub> and MoO<sub>3</sub>. This is in confirmation with past studies on the hot corrosion studies in molten salt environment on boiler tube steel [13].

The phase evolution of SS GP1 powder before and after corrosion was obtained by XRD analysis at the surface of the samples. The major peaks indicates the dominance of Fe, Cr, Ni. Figure 6 and 7 indicates the XRD analysis on laser sintered GP1 stainless steel surface before and after hot corrosion respectively

## 5. CONCLUSION

- Rate of oxidation was observed to be high in the early cycles of the study in the investigated environments, which may be attributed to the fact that during transient period of oxidation, the scales formed may be providing protection to the underneath metals.
- The accelerated hot corrosion was observed in the chloride+sulfate mixed molten salt environment in the form of intense spalling and sputtering of its scale.
- Rate of oxidation was observed to be high in the early cycles of the study in the investigated environments, which may be attributed to the fact that during transient period of oxidation, the scales formed may be providing protection to the underneath metals.
- The accelerated hot corrosion was observed in the chloride + sulphate mixed molten salt environment in the form of intense spalling and sputtering of its scale.
- Weight gain kinetics under air oxidation shows a steady-state parabolic rate law, whereas the molten salt environment is a multi-stage weight-gain growth rate

## References

1. Kurian Antony, Arivazhagan.N and Senthilkumaran.K .Numerical and experimental investigations on laser melting of stainless steel 316L metal powders. Journal of Manufacturing processes, 16 (2014), pp. 345–355.
2. Kurian Antony, Senthilkumaran.K, Dhana Govind Meda. The Effect of Neighborhood Scan Path Exposures on Heat Buildup: Numerical Investigations on the Laser Energy Delivery in Selective Laser Sintering Process, International Journal of Rapid Manufacturing, Vol. 4, Nos. 2/3/4, 2014.
3. Kurian Antony, Arivazhagan.N and Senthilkumaran.K .Studies on Wettability of Stainless Steel 316L powder in laser melting process. Journal of Engineering Science & Technology, 9, 5, 2014 ISSN 1823–4690.
4. Kurian Antony, Arivazhagan.N .Studies on energy penetration and marangoni effect during laser melting process. Journal of Engineering Science & Technology, vol.10,5,2015.
5. Kunal Prasad, Soumava Mukherjee, Kurian Antony, Manikandan M, Arivarasu M, Devendranath Ramkumar K, Arivazhagan N, Investigation on hot corrosion behavior of plasma spray coated nickel based super alloy in aggressive environments at 900°C. International Journal of Chem Tech Research, 6, 1, 416–431, 2014.
6. Kurian Antony, Arivazhagan.N and Senthilkumaran.K. Influence of laser melting process parameters on surface roughness behaviour for SS316L powder. Journal of Corrosion Science and Engineering, 16, 2013, ISSN 1466–8858.
7. Kurian Antony, Optimizing the Process Parameters for Laser melting of Stainless Steel Powders, International Journal of Applied Engineering Research , Volume 9, Number 24 (2014) pp. 28605–28610

8. Kurian Antony, Siva Prasad M. A Comparison of Corrosion Resistance of Stainless Steel Fabricated with Selective Laser Melting and Conventional Processing" International Journal of ChemTech Research, Vol.7, No.6, 2015.

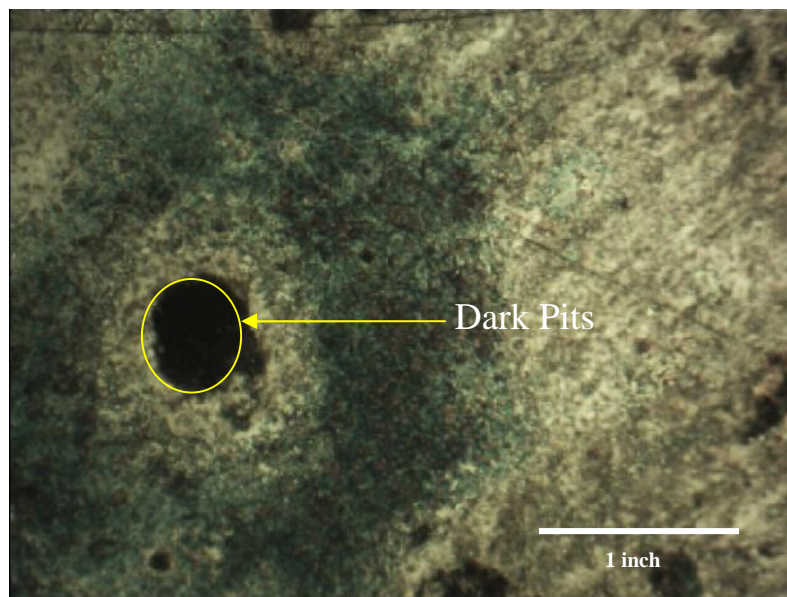


Figure1. Microstructure of corroded sample after 1 cycle.

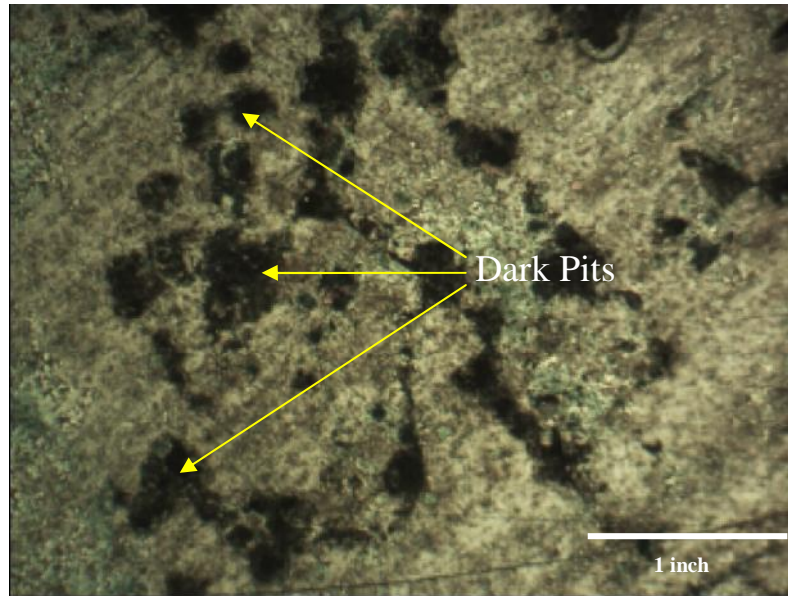


Figure 2. Microstructure of corroded sample after 1 cycle

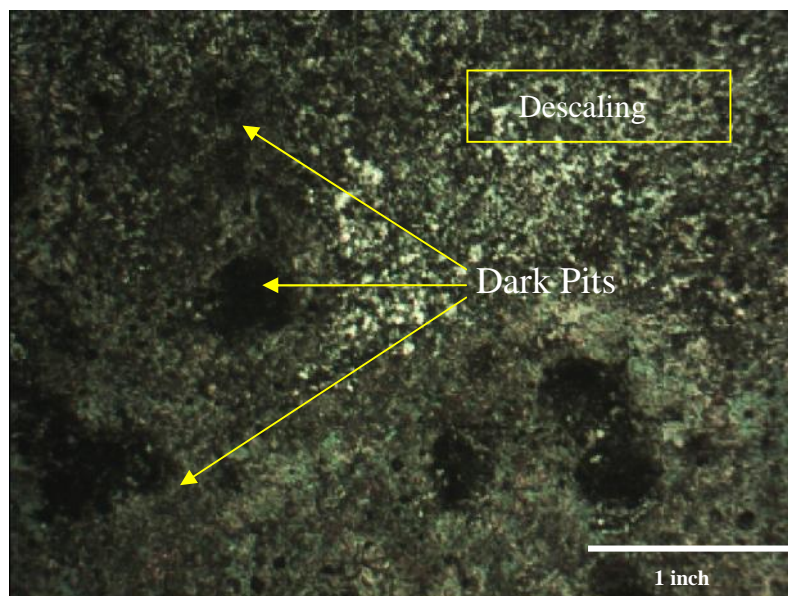


Figure3. Microstructure of corroded sample after 2 cycle



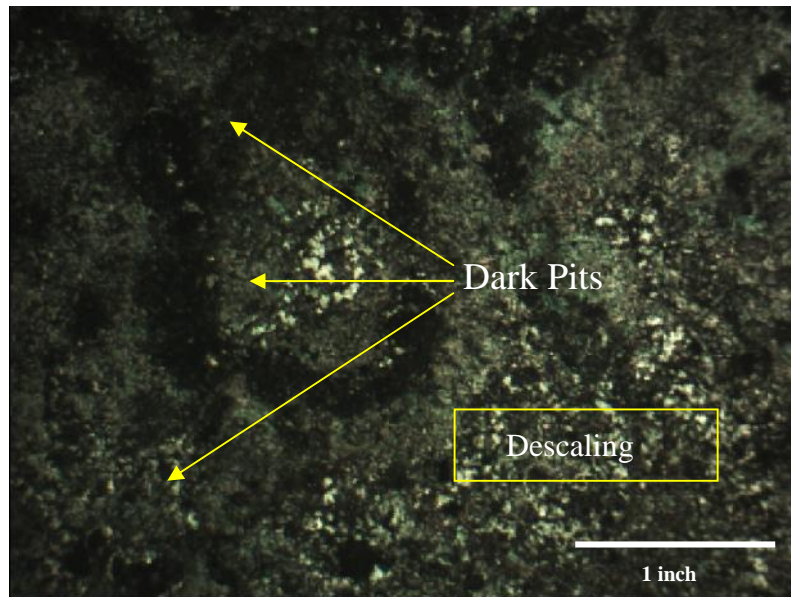


Figure4. Microstructure of corroded sample after 3 cycle

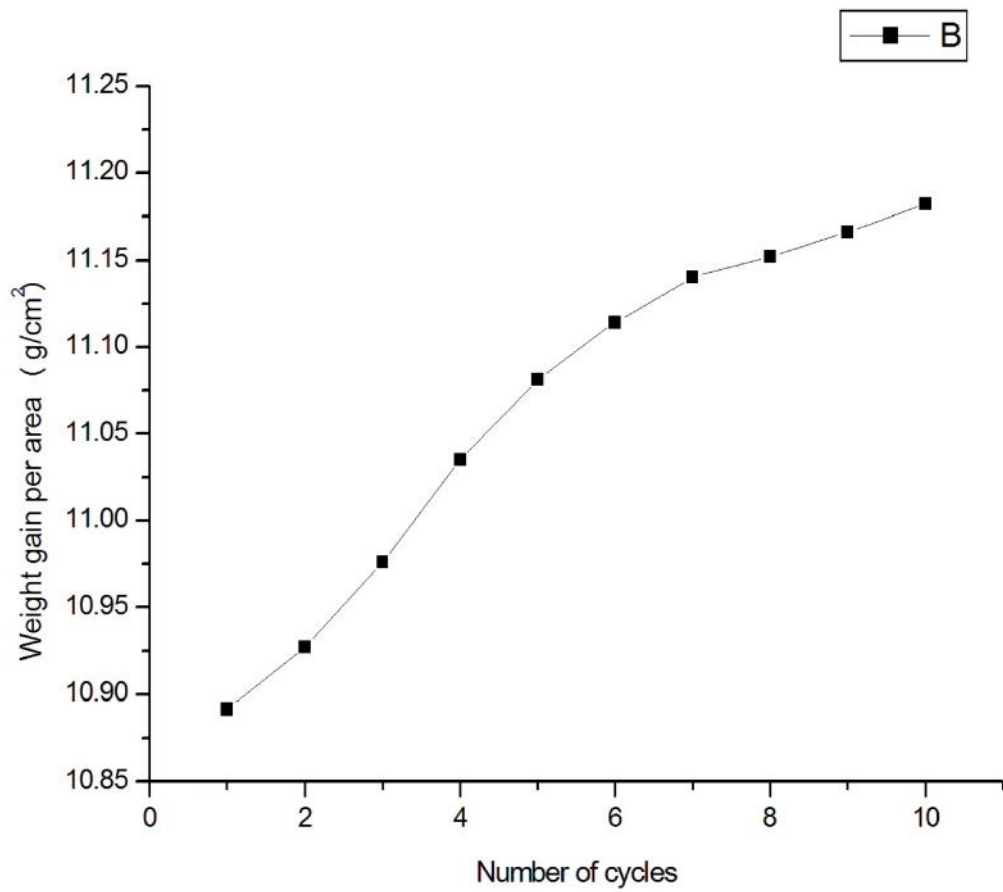


Figure5. Weight gain per area Vs Number of Cycles

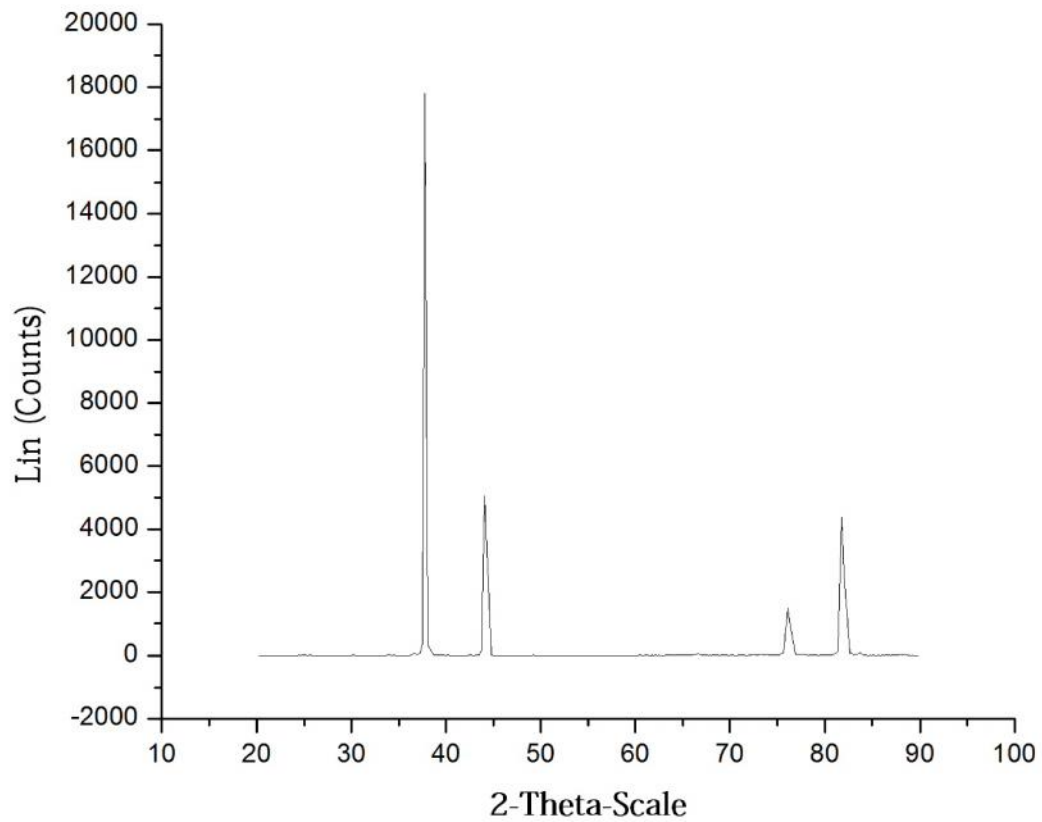


Figure 6. XRD analysis before corrosion

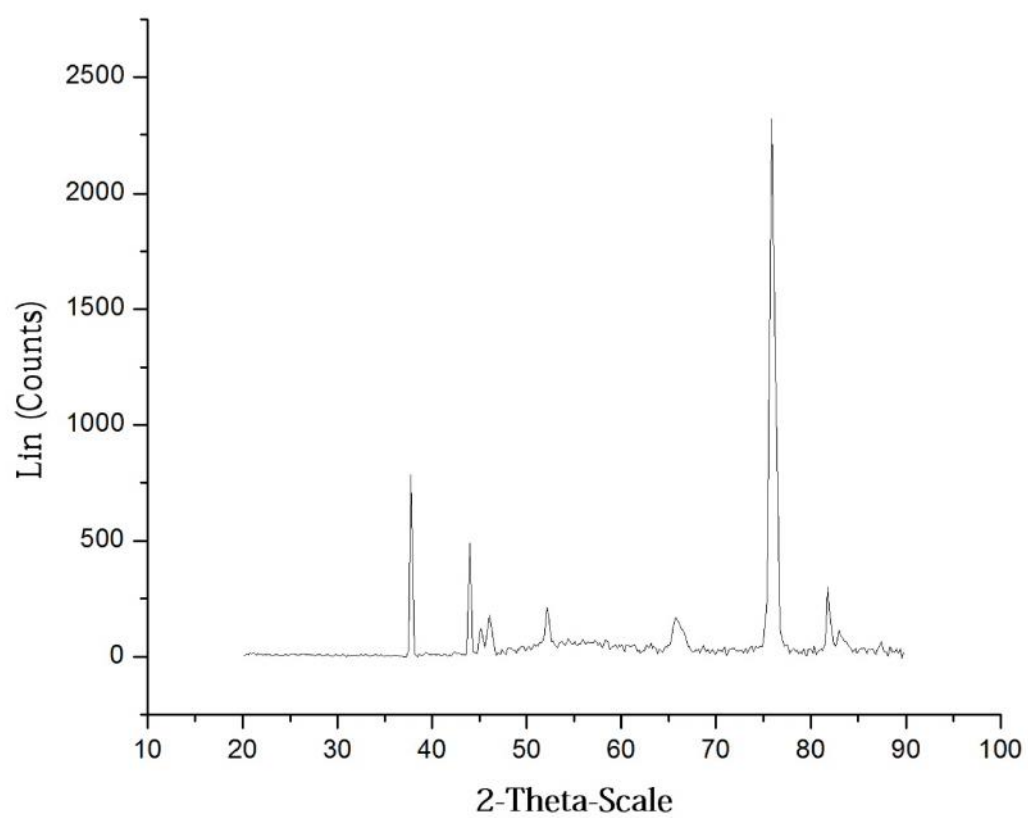


Figure.7. XRD analysis after corrosion